Langmuir

Article

pubs.acs.org/Langmuir

Adsorption Kinetics Dictate Monolayer Self-Assembly for Both Lipid-In and Lipid-Out Approaches to Droplet Interface Bilayer Formation

Guru A. Venkatesan,[†] Joonho Lee,[‡] Amir Barati Farimani,[‡] Mohammad Heiranian,[‡] C. Patrick Collier,[§] Narayana R. Aluru,[‡] and Stephen A. Sarles*[,†]

[†]Department of Mechanical, Aerospace, and Biomedical Engineering, University of Tennessee, Knoxville, Tennessee 37996, United States

[‡]Department of Mechanical Science and Engineering, University of Illinois at Urbana—Champaign, Urbana, Illinois 61801, United States

[§]Center for Nanophase Materials Sciences, Oak Ridge National Laboratory, Oak Ridge, Tennessee 37831, United States

Supporting Information

ABSTRACT: The droplet interface bilayer (DIB)—a method to assemble planar lipid bilayer membranes between lipid-coated aqueous droplets—has gained popularity among researchers in many fields. Well-packed lipid monolayer on aqueous droplet−oil interfaces is a prerequisite for successfully assembling DIBs. Such monolayers can be achieved by two different techniques: "lipid-in", in which phospholipids in the form of liposomes are placed in water, and "lipid-out", in which phospholipids are placed in oil as inverse micelles. While both approaches are capable of monolayer assembly needed for bilayer formation, droplet pairs assembled with these two techniques require significantly different incubation periods and exhibit different success rates for bilayer formation. In this study, we combine experimental interfacial tension measurements with molecular dynamics simulations of phospholipids (DPhPC and DOPC) assembled from water and oil origins to understand the differences in kinetics of monolayer formation. With the results from simulations and by using a simplified model to analyze dynamic interfacial tensions, we conclude that, at high lipid concentrations common to DIBs, monolayer formation is simple adsorption controlled for lipid-in technique, whereas it is predominantly adsorption-barrier controlled for the lipid-out technique due to the interaction of interface-bound lipids with lipid structures in the subsurface. The adsorption barrier established in lipid-out technique leads to a prolonged incubation time and lower bilayer formation success rate, proving a good correlation between interfacial tension measurements and bilayer formation. We also clarify that advective flow expedites monolayer formation and improves bilayer formation success rate by disrupting lipid structures, rather than enhancing diffusion, in the subsurface and at the interface for lipid-out technique. Additionally, electrical properties of DIBs formed with varying lipid placement and type are characterized.

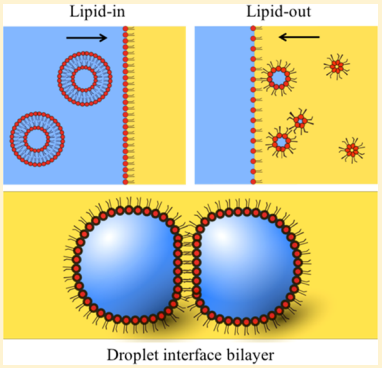

INTRODUCTION

Since its innovation in 2006,[1] the droplet interface bilayer (DIB) has been the basis for several innovative biomolecular material systems, such as membrane-based hair cell sensors,[2] biobatteries,[3] and electrical rectifiers,[4] and as characterization tools for proteins[5] and nanoparticles.[6] Due to its simplistic approach for forming durable lipid bilayers, DIBs have gained popularity among researchers of many disciplines. Forming a DIB involves simply connecting two lipid-coated aqueous droplets under a suitable organic solvent (a water-in-oil emulsion) to form a planar bilayer. This procedure relies on the amphiphilic nature of phospholipids that self-assemble into a lipid monolayer at the oil/water (OW) interface with their head-groups facing the water and tail-groups facing the oil.[7]

DIBs can be formed using two different approaches, known as "lipid-in" and "lipid-out," that differ in the placement of phospholipids in the multiphase system. Phospholipids are incorporated as liposomes into the aqueous droplets in the lipid-in approach, while, in the lipid-out technique, phospholipids are dispersed in the external oil phase in the form of inverse micelles. Both approaches seek to provide suitable conditions for assembling a lipid monolayer upon the diffusion and adsorption of lipids to the OW interface,[7] yet each has specific advantages in assembling planar lipid bilayers. For instance, asymmetric lipid bilayers with different lipid compositions in each leaflet of the bilayer can be formed with lipid-in technique,[8] but not with lipid-out technique in which a common lipid mixture is present in the oil surrounding all droplets. Also, a wider range of phospholipid types are known to form liposomes than dissolve in alkanes,[8] making the lipid-in technique amenable to more types of membranes, including complex mixtures.[9] However, the lipid-out technique

Received: June 23, 2015
Revised: November 2, 2015
Published: November 10, 2015

DOI: 10.1021/acs.langmuir.5b02293
Langmuir 2015, 31, 12883−12893

offers simpler preparation of lipid solution since dispersing lipids in oil avoids the need for freeze−thaw, extrusion, or sonication steps necessary for liposome preparation. Recent reports show that incorporation of saturated lipids into the oil phase allows for sufficient monolayer formation at room temperature,[10] whereas it is required to heat droplets containing liposomes with the same lipid to a temperature above the gel−liquid phase transition of the saturated lipid to enable sufficient assembly.[9] The lipid-out method also helps to maintain a lipid-free environment within the aqueous droplets that can be used to eliminate lipid and protein exchange between liposomes and interfacial bilayers and permit a wider range of chemical species in the droplet that may otherwise degrade liposomes.

From a bilayer formation standpoint, there are other differences. Lipid-in aqueous droplets (200−500 nL) can be routinely connected within 5 min of placing them in the oil,[7,9] unlike the lipid-out technique, in which 30 min or more is often required before the droplets can be brought into contact.[7,11,12] This time required between placing the aqueous droplets in oil and bringing them into contact during which the lipid monolayer assembles is called the *incubation period*. While monolayer assembly in the presence of contaminated oil or aqueous solutions, degraded lipids, or unclean substrates can all lead to droplet coalescence instead of bilayer formation, droplet coalescence is more often the result of insufficient incubation, especially in attempts to form DIBs with lipid-out technique that requires a longer incubation time. As a result, a lower bilayer formation success rate is reported with lipid-out technique when compared to lipid-in technique, especially in nonmicrofluidic devices.[11] The lower success rate of lipid-out DIBs has been explained qualitatively as being due to poor monolayer formation at the OW interface,[7] but the differences in phospholipid assembly from the oil phase has never been quantitatively characterized to identify why this approach is slower and less effective in promoting lipid organization. Abundant literature is available on stabilization of oil-in-water emulsion focusing on time required for self-assembly of surfactants such as sodium bis (2-ethylhexyl) sulfosuccinate (AOT) and sodium dodecyl sulfate (SDS) to reach a level of packing density that averts droplet fusion.[13−15] However, very few studies have been performed in regard to water-in-oil emulsions focusing specifically on the kinetics of phospholipid self-assembly for DIB formation.[16]

Thus, we identify that understanding the kinetics of lipid monolayer formation at an OW interface is important not only for DIB application, but also for other fields such as cosmetics, pharmacology, and food science where such water-in-oil emulsions are commonly used.[14,17] In this work, we study the self-assembly kinetics of phospholipids at an OW interface for both lipid-in and lipid-out water-in-oil systems to examine and quantify the fundamental differences in monolayer assembly. This work utilizes a combination of pendant drop experiments to measure the interfacial tension (IFT) at the OW interface and computational analysis to predict the molecular arrangements of phospholipids in two-phase liquid environments. We also study the effect of advective flow around the aqueous droplet on the rate and extent of self-assembly by providing intermittent stirring instead of a continuous flow in lipid-out cases.[16] DIBs obtained from these two techniques are characterized based on their electrical properties, including resistance and rupture potential, to explore differences in the resulting interfacial membranes. To our knowledge, this is the first attempt to characterize and compare the conditions required to form stable DIBs using lipid-in and lipid-out techniques. Two types of synthetic phospholipids that are widely used in the DIB community, namely 1,2-diphytanoyl-*sn*-glycero-3-phosphocholine (DPhPC) and 1,2-dioleoyl-*sn*-glycero-3-phosphocholine (DOPC) are considered in this study.[6,10,18,19] We discuss the differences in the monolayer formation rate for liposomes in water or inverse lipid micelles in hexadecane, the most widely used oil in DIB studies and identify reasons for slower monolayer formation in lipid-out cases.

MATERIALS AND METHODS

Lipid-In and Lipid-Out Solution Preparation. Lipids DPhPC and DOPC are purchased as lyophilized powders from Avanti Polar Lipids. In all lipid-in experiments, the aqueous volumes consist of 100 nm DPhPC or DOPC unilamellar liposomes in buffer (10 mM MOPS, 100 mM NaCl, pH 7), and the nonpolar phase is pure hexadecane oil ($C_{16}H_{34}$, 99%; Sigma-Aldrich). In all lipid-out experiments, the aqueous phase consists of buffer solution without liposomes, and the nonpolar phase includes inverse lipid micelles in hexadecane. Refer to SI for detailed solution preparation.

Interfacial Tension Measurement. Interfacial tension measurements are performed on hanging and inverted pendant droplets (see SI for details) using a pendant drop tensiometer (Ramé-Hart Instrument Co. Model 590) with a precision of 0.1 mN/m. To allow direct comparison, the droplet volume is maintained at 1 μL (unless mentioned otherwise) for both lipid-in and lipid-out cases. A minimum of 5 measurements is performed for all cases. Stirring of the bulk solution is performed in some tests using a magnetic stir bar (Sigma-Aldrich) and a custom magnetic stirrer positioned below the glass cuvette.

Bilayer Formation and Characterization. A PMMA substrate with an (height: 5 mm, width: 4 mm, depth: 8 mm each) open chamber is filled with nonpolar phase. 500 nL (unless specified otherwise) aqueous droplets are dispensed on wire-type silver−silver chloride (Ag/AgCl) electrodes that are mounted on micromanipulators (WPI). After appropriate incubation time, droplets are brought into contact to form a bilayer by manipulating the relative electrode positions. Bilayer electrical characterization is then performed using Axopatch 200B patch clamp amplifier (Molecular Devices). Detailed description of bilayer characterization is provided in the SI.

Computational Methods. In parallel to the experiments, we perform Molecular Dynamics (MD) simulations using GROMACS v.4.6.5 to study phospholipid self-assembly at the molecular level.[20] The recently developed GROMOS 53A6 force field is used to model the phospholipids.[21] GROMOS 53A6 force field is able to reproduce a broad range of lipid membrane properties. Water molecules are represented using the SPC/E model. The nonbonded interactions of phospholipid, oil and water are determined by Lennard−Jones parameters and electrostatic partial charges on molecules. The nonbonded interactions within 1.4 nm are calculated every step along with the pair list. Electrostatic nonbonded interaction is calculated by the Particle Mesh Ewald (PME) scheme.[22] A time step of 2 fs is chosen.

The simulation system setup is shown in Figure S4. The system consists of water, oil, phospholipids at the OW interface and a micelle (or an inverse micelle). Due to the limitations in the computational capabilities, micelles with 6 lipid molecules are modeled instead of liposomes that have ∼80 000 lipid molecules. The micelle (or inverse micelle) is initially located in the bulk region of the liquid environment (water or oil) a distance far away from the OW interface. Periodic boundary conditions are applied in all three spatial directions. The equilibration simulations are performed in the isothermal−isobaric (NPT) ensemble for 10 ns, with the direction perpendicular to the plane of the monolayer at OW interface coupled to 1 bar of pressure. The isothermal compressibility is set to 4.6×10^{-5} bar^{-1} and the coupling constant, τ_P, is set to 1 ps. The temperature of the system is

DOI: 10.1021/acs.langmuir.5b02293
Langmuir 2015, 31, 12883−12893

kept constant by independently coupling the lipids and solvent molecules to an external bath (T = 300 K) with a coupling constant of 0.1 ps using the Nosé-Hoover thermostat.[23] The micelle (or inverse micelle) is fixed in space during the equilibration.

After the equilibration, the simulations are extended further for 60 ns in the constant number of molecules, volume, and temperature (NVT) ensemble for the production runs. The micelle (or inverse micelle) is pulled toward the OW interface in both the lipid-in and lipid-out cases. The pulling speed and the spring constants are set at $v = 1.000 \times 10^{-5}$ nm/ps and $k = 1.686 \times 10^{3}$ kJ/mol nm^2, respectively. On the basis of the equilibrated configurations, we compute free energy profiles of the individual micelle and inverse micelle with respect to the distance from the OW interface.

RESULTS

Interfacial Tension Measurements. The interfacial tension of the neat hexadecane/water interface in absence of phospholipids is first measured to be 44 mN/m, consistent with the literature.[24,25] Figure 1 shows representative IFT data at the

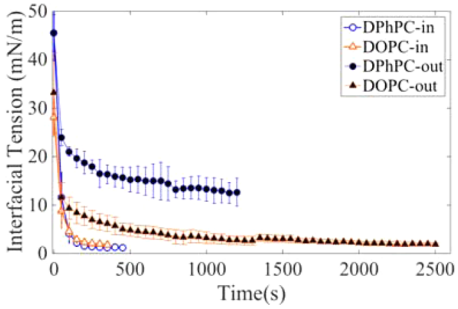

Figure 1. Interfacial tension versus time measured at an oil−water interface containing 2 mg/mL of either DPhPC or DOPC lipids placed in the aqueous buffer or hexadecane.

OW interface versus time for four different cases with phospholipids: DPhPC-liposomes (DPhPC-in) versus hexadecane, DOPC-in/hexadecane, DPhPC in hexadecane (DPhPC-out) versus aqueous buffer, and DOPC-out/buffer. In the cases of 2 mg/mL DPhPC-in and DOPC-in, the interfacial tension of a 1 μL aqueous droplet decreases rapidly from >40 mN/m to an equilibrium value of 1.18 ± 0.2 mN/m and 1.99 ± 0.5 mN/m (Table 1), respectively, within ∼300 s. The saturation suggests that DPhPC and DOPC molecules have assembled to form fully packed monolayers with surface pressures >42 mN/m (Surface pressure = IFT of pure OW interface − IFT of OW interface with self-assembled lipid; $\prod = \gamma_{O/W} - \gamma_{O/L/W}$).[26−28] On the contrary, equilibrium tensions are not reached within 20 min for the cases of DPhPC-out and DOPC-out at the same lipid concentration and droplet size. After an initially quick drop in tension during the first 50−100 s, a slower reduction in tension at a rate of about 0.04 mN/m/s or lower is observed for both lipid-out cases. At the end of 20 min, the IFT falls to 12 ± 2.0 mN/m for DPhPC-out and 2.7 ± 0.8 mN/m for DOPC-out. Equilibrium IFT of 1.8 ± 0.3 mN/m is recorded for DOPC-out within about 30 min, though an equilibrium tension is not obtained for DPhPC-out even at 1 h after droplet formation. These equilibrium tensions and rates for both lipid-in and lipid-out are in agreement with measurements of monolayer formation found in the literature.[10,16,27]

We performed a second series of experiments to examine the extent to which lipid concentration affects monolayer IFT for both lipid-in and lipid-out approaches. Figure S6a shows the change in interfacial tension as a function of time for three different concentrations of DPhPC liposomes (DPhPC-in) in the aqueous phase: 2, 0.2, and 0.002 mg/mL. All three concentrations are above the critical micelle concentration in water, which are in the ng/mL range for saturated phospholipids.[29] At 2 mg/mL concentration, an equilibrium tension of 1.5 mN/m is reached in less than 200 s, whereas at 0.2 mg/mL concentration, an equilibrium value of 1.86 mN/m is reached after only about 300 s. At a lower concentration of 0.002 mg/mL, the tension does not reach an equilibrium value even after 1000 s. Similarly, different concentrations of DPhPC-out display different rates of IFT reduction (Figure S6b), where again none of the lipid-out concentrations result in surface pressures >40 mN/m indicative of a fully packed monolayer.

Because inverse micelles are known to swell and form complex networks in oil with the addition of water[30,31] we also performed IFT measurements with intentionally aged and hydrated lipid-out solutions (0.1% v/v water content) to understand how these factors also may affect monolayer assembly. Results of the IFT measurements for fresh and freshly hydrated solutions of DPhPC-out and DOPC-out are compared in Figure S6d where no significant difference in rate of IFT reduction was noticed. In another set of experiments, intentionally aged lipid-out solutions were used to measure IFT (Figure S6c). A considerably lower rate of IFT reduction and much less dependence on concentration can be seen in case of the aged inverse micelle solutions compared to freshly prepared solutions.

As recently demonstrated by Thuttupalli et al., incorporating advective flow of the lipid-out solution around the droplet results in a large and rapid reduction in the IFT to a value of about 5 mN/m.[16] This is attributed to the flow-induced supply of fresh DOPC inverse micelles to the droplet subsurface. Therefore, a final series of IFT measurements were performed with stirring of the lipid-out solution to explore the effect of advective flow around the droplet on DPhPC-out monolayer formation. Figure 2a compares the IFT measurements of an aqueous droplet (1 μL) formed in still and intermittently

Table 1. Success Rates of DIB Formation and Measured Electrical Properties of the Bilayers

		DPhPC-in/hexadecane	DOPC-in/hexadecane	DPhPC-out/buffer	DOPC-out/buffer
eq monolayer tension (mN m^{-1})[b]		1.18 ± 0.2	1.99 ± 0.5	2.04 ± 0.15[a]	1.8 ± 0.3
bilayer formation success rate[c]	5 min	100%	0%	0%	40%
	20 min	100%	10%	5%	70%
	with flow	n/a	n/a	40%	100%
	hydrated	n/a	n/a	5%	80%
electrical properties[d]	specific resistance (MΩ-cm^2)	8.04 ± 3.6	0.55 ± 0.25	1.7 ± 0.8	0.7 ± 0.22
	max. rupture potential (mV)	275	150	100	125

[a]Equilibrium interfacial tension reached after stirring. [b]1 μL droplets. [c]500 nL droplets. [d]500 nL droplets (except 200 nL for DOPC-in/hexadecane).

DOI: 10.1021/acs.langmuir.5b02293
Langmuir 2015, 31, 12883−12893

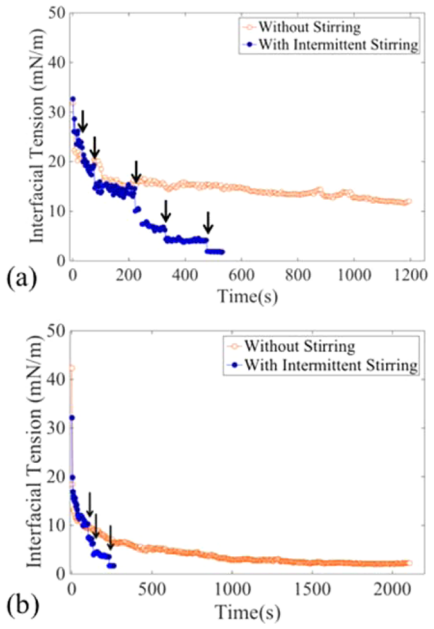

Figure 2. Interfacial tension versus time: (a) 2 mg/mL DPhPC-out with and without stirring and (b) 2 mg/mL DOPC-out with and without stirring the lipid-out solution for a 1 μL droplet. Arrows mark the beginning of 30 s periods of stirring.

stirred hexadecane containing 2 mg/mL DPhPC. An IFT value of 10 mN/m is reached after about 2000 s in a still bulk solution, while an equilibrium value of 1.9 mN/m is reached within 600 s with five periods of stirring (30 s each) of the bulk solution. Similar behavior is seen in DOPC-out solution (Figure 2b).

DIB Formation versus Lipid Type and Placement. DIB formation success rates under various conditions with a lipid concentration of 2 mg/mL are presented in Table 1. With DPhPC-in, a near 100% DIB formation success rate is seen when 500 nL droplets are placed in contact after a 5 min incubation time in hexadecane. Meanwhile, tests with DOPC-in droplets in hexadecane rarely form stable lipid bilayers, usually rupturing immediately upon contact even when connected after 20 min of incubation time in oil. Interestingly, a significant increase in DIB formation success rate is observed for DOPC-in when smaller droplets (<200 nL) are used.

In sharp contrast, aqueous droplets of buffer solution placed in DPhPC-out oil yield bilayers in only 5% of the trials after 20 min of incubation. This result holds true for lipid concentrations ranging from 0.2 mg/mL to 10 mg/mL in still oil; however, as many as 60% of trials with DPhPC-out lipid solution yielded stable lipid bilayers after only 10 min when the droplets are tossed back and forth in a tube containing the same lipid-out solution as reported elsewhere.[3,11] Comparable success rates (40%) are seen herein when a similar flow mechanism is implemented to prime the droplets. Separately, aqueous droplets placed in fresh DOPC-out and hydrated DOPC-out solutions are able to form DIBs with high success rates (70% and 80%, respectively) when connected within 20 min. Measured electrical properties (Table 1), contact angles and calculated bilayer tensions and energies of adhesion (provided in Table S1) fall in expected ranges as reported in the literature.[10,32]

Simulation Results. First, the changes in free energy of an individual DPhPC micelle and, separately, a DPhPC inverse micelle near a pristine OW interface (without any pre-existing lipid molecules at the interface) are computed via MD. The calculated potential profile, based on the Jarzinsky relation,[33] is symmetrized about z = 0 (the OW interface) such that the potential is zero when the micelle (or inverse micelle) is in the bulk liquid environment (oil or water) on either side of the interface. The free energy curves of the micelle (Figure 3a) and the inverse micelle (Figure 3b) indicate the relative favorability of lipid-in and lipid-out micelles to self-assemble at the OW interface. The potential of a 6-lipid micelle in water at the interface with respect to the bulk is −450 kJ/mol, while, for an inverse micelle (lipid-out) of the same size, the magnitude of the potential well at the interface is ∼105 kJ/mol. This four times stronger potential field near the interface in DPhPC-in case compared to DPhPC-out assembly case gives rise to faster and more favorable self-assembly at a pristine OW interface. Comparable free energy curves are observed for DOPC-in and DOPC-out cases as well (Figure S9).

In order to investigate the effects of pre-existing lipid molecules at the OW interface on the self-assembly (i.e., a partially packed interface), a second set of MD simulations are performed in which the OW interface is occupied by a sparsely packed monolayer. The population of pre-existing lipid molecules at the OW interface is controlled to establish various levels of defined initial configurations for the production runs. Four different packing density (area per lipid) cases of sparse lipid monolayers are examined: 2.54 nm^2/#, 1.45 nm^2/#, 1.02 nm^2/#, and 0.79 nm^2/#, where 0.79 nm^2/# corresponds to a surface pressure of 40 mN/m—maximum packing density reported in literature for DPhPC.[34] Represented in terms of percent coverage, 0.79 nm^2/# corresponds to 100% coverage, and 2.54 nm^2/#, 1.45 nm^2/#, and 1.02 nm^2/# correspond to

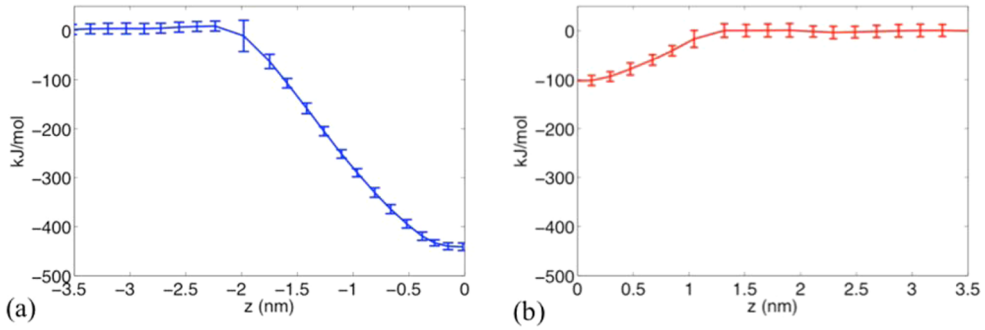

Figure 3. DPhPC lipid assembly: Free energy curves for (a) the micelle (lipid-in) and (b) the inverse micelle (lipid-out) as a function of the distance from the pristine OW interface. Refer to Figure S9 for DOPC assembly free energy curves.

DOI: 10.1021/acs.langmuir.5b02293
Langmuir 2015, 31, 12883−12893

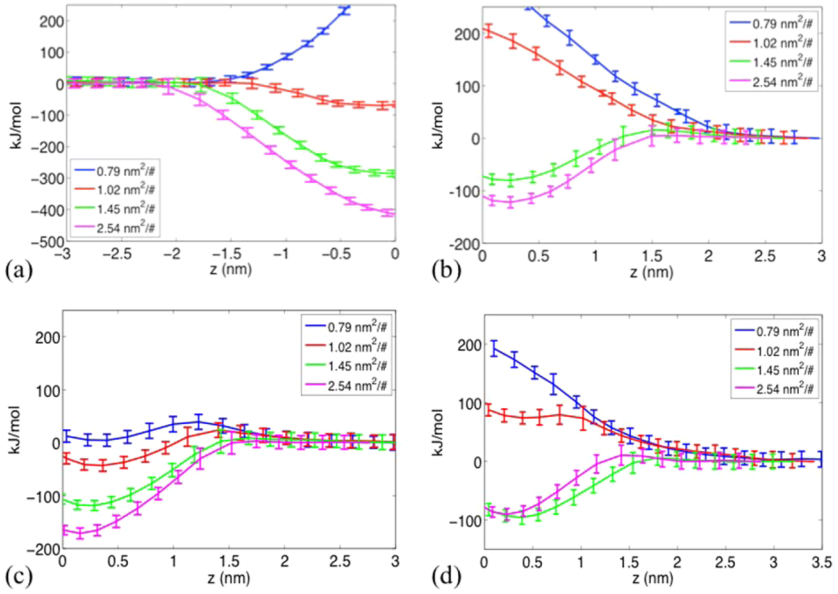

Figure 4. Free energy curves for (a) DPhPC-in micelles, (b) DPhPC-out inverse micelles, (c) DOPC-out inverse micelles, and (d) DPhPC-out swollen inverse micelles w.r.t. the distance from the OW interface with different packing density monolayers.

31%, 54% and 77% coverage, respectively. The resultant free energy profiles for self-assembly process are compared in Figure 4. The potentials of the micelle at the OW interface are favorable (negative free-energy with respect to that of the bulk) for 2.54 nm^2/#, 1.45 nm^2/#, and 1.02 nm^2/#, and unfavorable for 0.79 nm^2/# in the lipid-in case (Figure 4a). In other words, the micelles in water can spontaneously assemble at the interface to form a tightly packed monolayer until the maximum packing density is reached. However, inverse micelles in the lipid-out case display a positive potential (unfavorable) for a packing density as low as 1.02 nm^2/# despite the fact that there is enough space at the interface for more lipid molecules to insert (Figure 4b). These results indicate clearly that sparsely packed lipid monolayers with low area per lipid significantly hinder adsorption of lipid molecules assembling from the oil (lipid-out).

Additionally, the lipid-out self-assembly for the two types of lipid molecules (DOPC and DPhPC) are compared. The free energy curve of the DOPC-out (Figure 4c) shows stronger potential wells at the interface compared to the DPhPC case (Figure 4b), which indicates that the DOPC self-assembly is energetically more favorable than DPhPC-out assembly. These results explain the difference in the speed of the DPhPC-out and DOPC-out self-assembly that was observed in the experiments (Figure 1). Free energy curves for DOPC-in are not estimated as the IFT dynamics of DOPC-in are very much comparable to DPhPC-in. Therefore, drastic differences are not expected.

Finally, to understand the effect of hydrated (swollen) inverse micelles on the change in free energy during self-assembly, simulations are performed with 35 water molecules between the head groups of an inverse micelle. The free energy in the 1.02 nm^2/# and 0.79 nm^2/# cases still exhibit positive values (i.e., unfavorable) near the interface as shown in Figure 4d, but the magnitudes of the free energy barriers at the interface are reduced compared to the unhydrated case. Similarly, in the 1.45 nm^2/# case, self-assembly of a hydrated inverse micelle is slightly more favorable than its unhydrated form. This result is also in agreement with the experimental results (Figure S6d).

DISCUSSION

When an aqueous droplet is placed in a nonpolar solvent such as hexadecane, an interfacial tension is experienced at the droplet surface due to the relative strengths of attractive and repulsive van der Waals forces among oil molecules and water molecules. Lipid molecules, like other surfactants, self-assemble at the OW interface to reduce this interfacial tension, thereby lowering the surface free energy of the system. When these molecules form tightly packed monolayers, the IFT drops from ~44 mN/m ($\gamma_{O/W}$) to ~1−2 mN/m ($\gamma_{O/L/W}$), a minimum tension that corresponds to a maximum surface pressure ($\Pi = \gamma_{O/W} - \gamma_{O/L/W}$) value >40 mN/m.[17,26,27,29] We measured the change in IFT over time at an OW interface caused by lipid self-assembly for two different lipids (DPhPC and DOPC) placed in two different liquid phases (water and hexadecane) using pendant drop tensiometry.

In general, we observed 5X and 10X slower rates of lipid monolayer formation for DOPC and DPhPC, respectively, when the lipids assemble at the interface from the oil phase versus from the aqueous side. Using MD simulations, we calculated a significantly higher (4X) decrease in free energy for DPhPC-in micelles compared to that for DPhPC-out inverse micelles. Similar magnitudes of energetic favorability are seen for DOPC-in when compared to DOPC-out as shown in Figure S9.

The free energy includes different components, namely the lipid−water, lipid−oil, and lipid−lipid interaction energies which are a function of the parameters for the Lennard-Jones (L-J) and Coulombic interactions. In the case of DPhPC and DOPC, the fact that the L−J parameters and the lipid charge distributions (DPhPC with 38 and DOPC with 24 charged atoms) are different gives rise to the differences observed in the free energy profiles. Note that the computed free energy includes both electrostatic and L−J contributions. When the lipid micelles in water (lipid-in) move toward the OW interface, they are surrounded by more water molecules than by oil

DOI: 10.1021/acs.langmuir.5b02293
Langmuir 2015, 31, 12883−12893

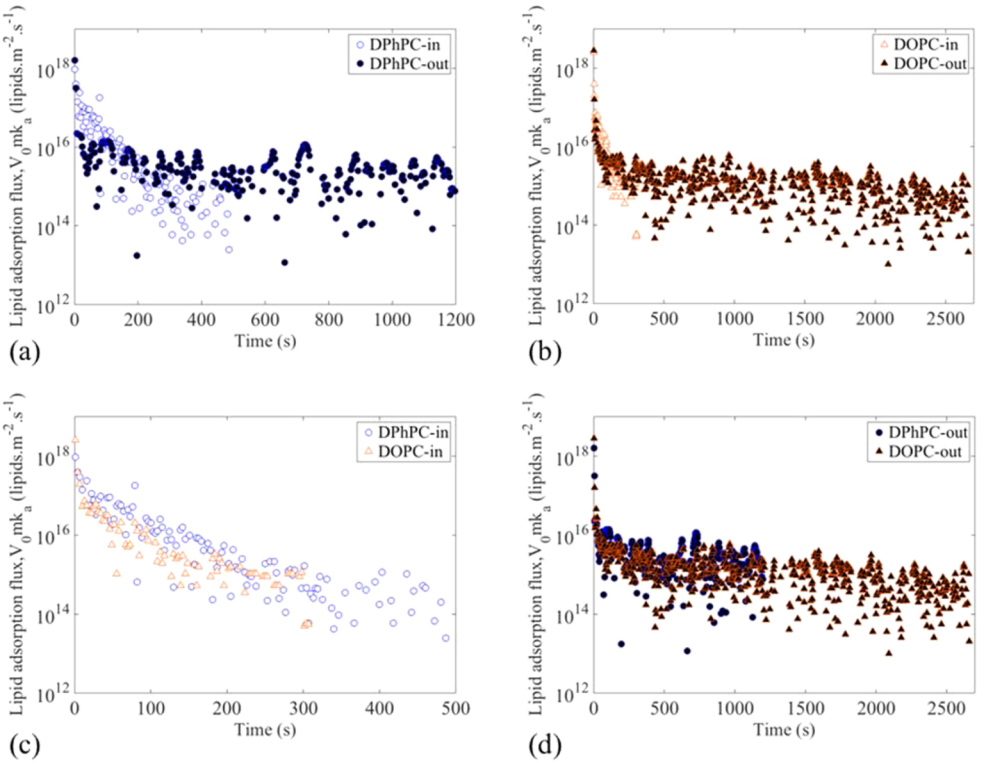

Figure 5. Estimated lipid adsorption flux versus time for (a) DPhPC-in and DPhPC-out, (b) DOPC-in and DOPC-out, (c) DPhPC-in and DOPC-in, and (d) DPhPC-out and DOPC-out at 2 mg/mL concentration. Note: Only nonzero values are plotted.

molecules (and the opposite for lipid-out method). This results in stronger lipid−water interactions for the lipid-in case resulting in a different energy profile from the lipid-out case. These results confirm that rates and energetics of assembly are not equal for lipids approaching the OW water interface from opposite sides, respectively.

In reviewing the literature, we found several studies[35−40] that examined the kinetics of monolayer formation at a polar-nonpolar fluid interface (e.g., water−air, water−oil) from liposomes distributed in the aqueous phase. These works contribute a basic understanding of the assembly process that consists of serial diffusion (liposomes diffuse from the bulk to the subsurface) and adsorption steps (vesicle structure in the subsurface disrupts and lipids assemble at the interface).[39,41] The total rate of monolayer formation is thus limited by the slower of these two serial steps. When the concentration of liposomes in the bulk is quite low (<2 μM), the rate limiting process is reported to be the diffusion of liposomes into the subsurface (i.e., relatively fast adsorption acts to continually deplete the subsurface such that monolayer formation requires waiting on the next liposome to diffuse).[29] However, when the bulk liposome concentration is high enough (>0.2 mM), diffusion is the faster of the two steps. Furthermore, our calculations show that for ∼0.2 mM concentration, less than 4% of the total lipid present in the droplet is required for a fully packed monolayer (refer to Table S2).

In our study, concentrations of lipids in the two liquid phases ranged from the typical concentration of ∼2 mM used for forming DIBs down to ∼2 μM. The computed values of the diffusion coefficients[35] of both 100 nm-diameter liposomes in water (1 cP viscosity) and 10 nm-diameter inverse micelles in hexadecane (3 cP) are found to be quite similar: 4×10^{-12} m^2/s for the liposomes and 7×10^{-12} m^2/s for the inverse micelles. Therefore, we realize that the differences in kinetics of monolayer formation between lipid-in and lipid-out must not arise from the difference in diffusion of liposomes and inverse micelles. Instead, the differences must originate from differences in adsorption of lipid structures from subsurface.

Differences in lipid adsorption for the two approaches are quantified using a first-order irreversible reaction model to empirically extract short-term rates of adsorption. In this model, the concentration of lipids in the subsurface, C_0 (mol·m^{-2}) is considered as the reactant while the surface density of phospholipids, Γ (mol·m^{-2}), is the product as shown in the following scheme, where k_a is considered to be a time varying adsorption rate constant (s^{-1}):

$$C_0 \xrightarrow[k_a(t)]{} \Gamma \tag{1}$$

Due to high diffusion rates and high bulk lipid concentrations used in our system, C_0 is considered to be constant.[28] For irreversible adsorption, the rate of increase in surface density of lipids in the monolayer is written as follows:

$$\frac{d\Gamma}{dt} = k_a(t)C_0 \tag{2}$$

For short time intervals (i.e., those much less than the time required for the surface tension to equilibrate), where the k_a is assumed to be a constant, integrating eq 2 yields a linear temporal solution for the surface density of lipids in the monolayer. This solution can be rewritten in terms of the liposome (or inverse micelle) areal density in the subsurface, V_0 (liposomes·m^{-2} or inverse micelles·m^{-2}), and the number of lipids per unit structure, m, (i.e., 80 000 lipids/liposome or 100 lipids/invers micelle) as follows:

DOI: 10.1021/acs.langmuir.5b02293
Langmuir 2015, 31, 12883−12893

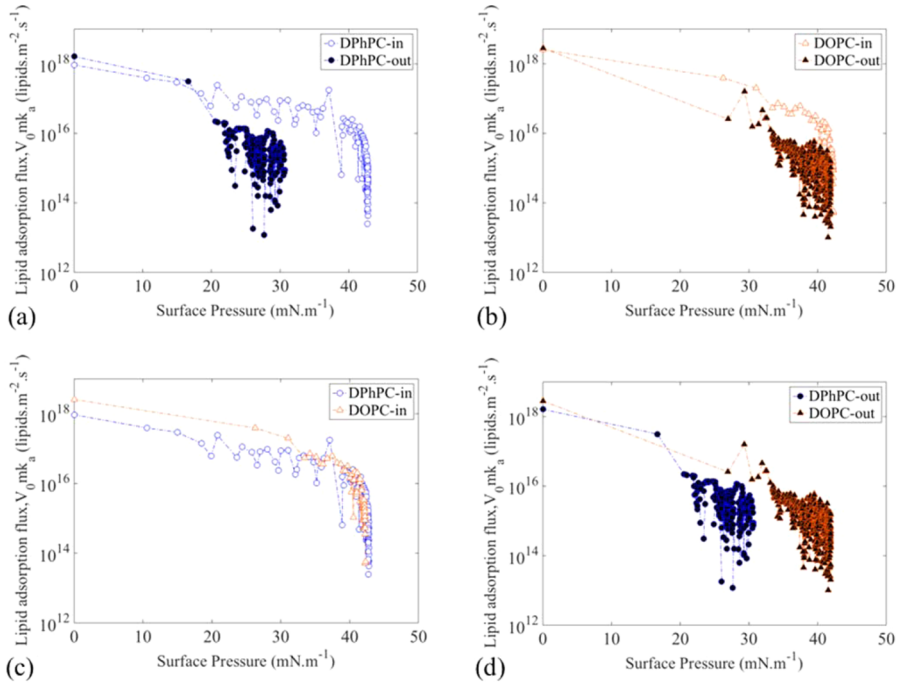

Figure 6. Estimated lipid adsorption flux versus surface pressure for, (a) DPhPC-in and DPhPC-out, (b) DOPC-in and DOPC-out, (c) DPhPC-in and DOPC-in, and (d) DPhPC-out and DOPC-out at 2 mg/mL concentration. Note: Only nonzero values are plotted. See additional note in the SI.

$$\Gamma(t) = \frac{V_0 m}{A_v} k_a t \tag{3}$$

where A_v is Avogadro's number (6.02×10^{23} molecules/mol). At short times, eq 3 shows a linear relationship between the time varying surface concentration and subsurface lipid concentration, adsorption rate, and time. Finally, an equation of state is required to relate surface density of lipids to surface pressure. Henry's surface equation of state relates equilibrium surface concentration to surface pressure, Π:[42]

$$\Pi(t) = nRT\Gamma(t) \tag{4}$$

where R is the ideal gas constant (mJ·mol^{-1}·K^{-1}), T is the absolute temperature (K), and n is a factor that depends on the type of surfactant (n = 1 for nonionic surfactants, n = 2 for ionic surfactants). Thus, for neutral lipids like DPhPC and DOPC, n = 1. Equation 4 is valid for low surfactant concentration systems where interaction between adsorbed surfactants is assumed to be negligible.[43] As suggested by Bleys et al., equilibrium eq 4 can be applied to a dynamic system.[44] Thus, substituting eq 3 into eq 4 yields the following linear relationship for surface pressure versus time for irreversible adsorption at a fixed adsorption rate during brief intervals:

$$\Pi(t) = \frac{RT}{A_v} V_0 m k_a t \tag{5}$$

Yet, IFT measurements of phospholipids at an OW interface (Figure 1) clearly show that surface pressure does not increase linearly with time. To account for the fact that measured surface pressures converge nonlinearly to a final value, we consider that the favorability for lipid adsorption must decrease as surface density rises due to (1) decreasing available area at the interface for new lipids[39] and (2) inhibiting interactions between adsorbed molecules and those in the subsurface.[43]

Empirically, this slowing of adsorption is captured by a decrease in the adsorption rate constant, k_a, or in the lipid adsorption flux represented by the product $V_0 mk_a$. By letting the product mk_a vary during the measurement, eq 5 can thus be used to fit nonlinear IFT data well in successive, 4 s time segments during which a local rate constant (mk_a) is computed from the slope (Figure S7b). The resulting dynamics of rates for both the lipid types placed in either phase are shown in terms of lipid adsorption flux, $V_0 mk_a$ (lipids·m^{-2}·s^{-1}) in Figure 5. After the first few seconds of fast adsorption, the lipid adsorption flux abruptly drops down and adsorption continues at a slower flux for DPhPC-out (Figure 5a). Such distinct change in lipid adsorption flux—a high initial flux followed by drastically slower flux until equilibrium is reached—is seen for both DPhPC-out and DOPC-out after about 75 s (Figure 5d). Dynamics of lipid adsorption flux for both DPhPC-in and DOPC-in does not seem to display such distinct regimes; rather, a linear decline of lipid adsorption flux (Figure 5c) is noticed. A noticeable difference in adsorption behavior for lipid-out suggests the possibility of the onset of an additional adsorption barrier leading to a changeover in regimes.

To further investigate the differences, data from Figure 1 and Figure 5 are combined in Figure 6 to cast the progression of lipid adsorption flux in terms of increasing surface pressure, which is proportional to surface density. As expected, in both lipid-in and lipid-out techniques, the lipid adsorption flux is highest during the first few seconds of monolayer formation when the surface pressure is the lowest as the lipid structures encounter a "clean" OW interface. During this phase, one could assume complete rupturing of liposomes or inverse micelles to deposit its entire content at the interface. Walker and Richmond explained this as the "rupture mechanism" (Figure 7a,c).[28,39] The higher initial values for lipid-in when compared to their lipid-out counterparts is possibly due to, (a) the difference in the tendencies of liposomes and inverse micelles to break open at the interface, and (b) the difference between the number of lipids per liposome (~80 000 molecules) and an inverse micelle (~100 molecules).

DOI: 10.1021/acs.langmuir.5b02293
Langmuir 2015, 31, 12883−12893

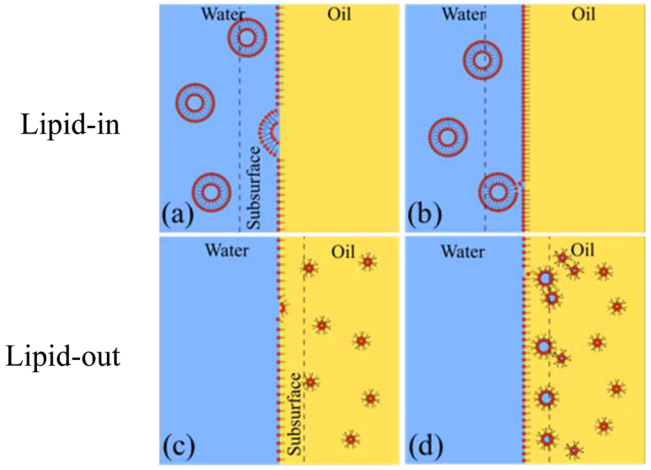

Figure 7. Schematic representation of lipid self-assembly at an oil–water interface following rupture mechanism (a, lipid-in; c, lipid-out) and extraction mechanism (b, lipid-in; d, lipid-out). Schematic (d) depicts the swollen inverse micelles through uptake of water.

As the surface concentration of lipids increases, the lipid adsorption flux starts to reduce due to the diminished exposed-OW interface and increasing repulsive interaction between the adsorbed lipids and the lipid structures approaching the interface. Figure 6c shows that, for DPhPC-in and DOPC-in, such hindrance (quantified as low lipid adsorption flux) is minimal until the surface pressure reaches close to the maximum value (>40 mN/m) where the exposed-OW interface is minimal. On the contrary, for DPhPC-out, such an adsorption barrier intensifies at a much lower surface pressure (~23 mN/m) and hinders further adsorption (Figure 6a). Hence, a much slower reduction in surface tension is noticed after the initial quick drop in IFT (Figure 1). A similar adsorption barrier is seen in DOPC-out although only after a relatively higher surface pressure (~35 mN/m) is reached, which is possibly due to higher fluidity of DOPC tail groups when compared to DPhPC.[45,46] We hypothesize that once this adsorption barrier has been established (2nd regime in Figure 6), adsorption takes place via an "extraction mechanism" (Figure 7b,d)—the process by which liposomes or inverse micelles deposit a fraction of its lipid content into the interface while remaining intact[28,39]—rather than by rupture mechanism. In agreement, the MD simulations show that an increase in free energy is observed when a DPhPC inverse micelle is placed near a partially packed interface with packing densities as high as 1.02 nm^2/# (Figure 4b). In other words, adsorption of lipid molecules into the interface is hindered before the packing density of lipids at the interface reaches the maximum value of 0.79 nm^2/# as seen in lipid-in. Therefore, we arrive at the conclusion that after a short period of simple adsorption-controlled process, such adsorption barriers limit the continued process of lipid self-assembly at the interface for lipid-out technique. In contrast, analysis of the lipid-in IFT data indicate that such adsorption barriers are not encountered for lipid-in until maximum packing density is achieved as the liposome–monolayer interaction is repulsive[47]—for comparison purposes, we call this a simple adsorption-controlled process. Furthermore, we conclude that diffusion is not a rate-controlling step due to the high concentrations used in our study for both lipid-in and lipid-out. In agreement, such mixed diffusion, adsorption, and adsorption-barrier controlled self-assembly have also been reported for phosphatidylcholine and other micelle forming surfactants at an OW interface.[29,48−51]

One possible explanation for the onset of the adsorption barrier for inverse micelles is the formation of hydrated-inverse micelles and lipid-based organogels in the subsurface of the lipid-out solution.[30] The incorporation of water (0.1% v/v) into a nonpolar organic solvent containing a high concentration of lipids is found to have substantial effects on both the nanoscale self-assembly of the lipids as well as the bulk properties of the solution.[30] For example, hydrating inverse micelles can result in the formation of worm-like structures that can overlap to form three-dimensional networks.[52] Upon hydration, drastic increase in the size of lipid structures is measured using DLS (Figure S5). However, both experimental and MD simulation results show that there is no drastic, adverse difference in the rate of IFT reduction and energetic favorability for swollen inverse micelles over their unswollen counterparts (Figure S6.d). While these structures do not drastically affect the monolayer formation, these tangled micellar structures, may affect the bilayer formation. Although our MD simulations do not show evidence for aggregation of inverse micelle to the partially packed monolayer, the possibility of forming multimolecular layers tethered to such interface should not be neglected.[29,50,53,54]

Our experiments and others have shown that stirring lipid-out solution increases the packing density of lipids at an OW interface by providing an advective flow of species around the aqueous droplets. In prior works, the enhanced rate of assembly was attributed to a reduction in the time required for the lipid species to reach the interface.[16] Quicker self-assembly of lipids is seen in microfluidic devices than in a static system due to the convective motion of the droplet and the bulk that is found in the former system.[13,16] This difference was attributed to the advection-induced transport of lipids to the interface. Self-assembly studies using fluorescent surfactants in microfluidic devices displayed a decreasing concentration gradient of the adsorbed lipids from the rear to the front of the droplet that is in motion due to the presence of shear flow.[13] Having proven the propensity of lipid-out systems to exhibit adsorption-limited kinetics, we believe that flow may actually have multiple roles: (a) to crowd the assembled lipids at the interface due to shear flow, exposing bare OW interface where lipids in subsurface can get adsorbed (promoting rupture mechanism rather than extraction), and (b) to perturb lipid assembly in the subsurface due to advective flow, allowing additional lipid insertion, thus reducing the IFT. Such stirring induced reduction in IFT is seen in both DOPC-out and DPhPC-out techniques (Figure 2). Stirring did not have drastic effects on "aged" or "hydrated" lipid-out solutions (data not shown) as presence of complex lipid structures in the bulk could affect the self-assembly process drastically.

Differences between DPhPC and DOPC IFT reduction rate could be due to the different innate shape of the lipids, the bulky methyl groups on the acyl chains of DPhPC, or the difference in phase of lipid at 20 °C (phase transition temperature, t_m for DOPC: −18 °C; t_m DPhPC: no transition between −120 to 120 °C).[46] DOPC-out inverse micelles, unlike DPhPC-out, do not exhibit an increase in free energy when placed near a packed interface with area per lipid as low as 0.79 nm^2. This is likely because DOPC molecules occupy a lower area (~65 nm^2/#) at its maximum packing density.[55] Prepacking the interface with a more tightly packed monolayer could produce a positive change in free energy.

DOI: 10.1021/acs.langmuir.5b02293
Langmuir 2015, 31, 12883−12893

To summarize, tightly packed monolayers are obtained within 5 min of droplet formation for both DPhPC-in and DOPC-in, and in about 30 min for DOPC-out. However, such tightly packed monolayer is not achieved with DPhPC-out even after 1 h. We attribute this to the adsorption barrier established due to the presence of aggregated and/or hydrated inverse micelles interacting with the partially packed monolayer. Nevertheless, stirring of the bulk lipid-out solution are found to help achieve tightly packed monolayer quickly. We accredit this to the convection-induced relocation of interface-bound lipids and restoration of rupture mechanism based adsorption.

For bilayer formation, priming droplets with such flow techniques is not required for lipid-in solutions, since a tightly packed monolayer assembles within 5 min, and monodispersed liposomes do not aggregate with one another or with the monolayer over time (see Figure S5).[47] This favorability translates into a near 100% bilayer formation success rate seen in the case of DPhPC-in. While a similar behavior is expected from DOPC-in (as the IFT reduced to near 1.99 mN/m within 5 min), droplets (>200 nL) with DOPC liposomes fail to form DIBs with high success rate even when connected after 20 min or longer. Nevertheless, smaller droplets (<200 nL) seem to form DIBs even within 5 min with a drastically higher rate.[19,56] The reason for such droplet size-dependent behavior is unclear and requires separate investigation; varying monolayer Laplace pressures, droplet curvatures, and lipid shape factors may all be responsible.[57] As expected from the measured IFTs, low bilayer formation success rate is seen for DPhPC-out and DOPC-out when connected within 5 min, and higher success rate for DOPC-out after a 20 min incubation time.

In accordance with the IFT data for hydrated DOPC-out (Figure S6d), a significantly higher success rate and reduced required incubation time is observed when connected just after 10 min. However, hydrated DPhPC-out, in stationary conditions, did not seem to improve the success rate. Employing a flow mechanism to prime the droplets before connecting improved the success rate for DPhPC-out considerably, which we explain by relocating the hydrated inverse micelles and other complex lipid structures away from the droplet subsurface, which can be found in stationary systems. In summary, near 100% DIB formation success rate displayed by DPhPC-in (which has the quickest monolayer formation rate) and the dependence of success rate on droplet size for DOPC-in and hydration level for DOPC-out and DPhPC-out proves that while tightly packed monolayer is a fundamental precondition, it is not the only requirement.

High electrical resistance (gigaohm) allows detection and characterization of single-channel membrane proteins and peptides that are inserted in the bilayer. Bilayers with higher rupture potential (>125 mV) are favorable for studying voltage-regulated species such as alamethicin. DIBs formed with DPhPC-in are found to have both of these desired properties. DIBs formed with other three cases seem to have low rupture potentials (<125 mV). Bilayers formed with DOPC in either phase appear to have lower resistance when compared to bilayers formed with DPhPC. This difference in bilayer resistance, again, could be because of the difference in shape factor and fluidity of these two lipids at room temperature. Measured specific capacitance values (Table S1) for DPhPC and DOPC bilayers match the values reported in literature,[58,59] and no drastic difference is noticed between the bilayers obtained from the same lipid type placed in different phases. This confirms that the hydrophobic thickness of bilayers obtained from the same lipid type is not affected by the phase in which the lipids are placed.[60] The consistency in contact angle (Table S1) across the various configurations is explained by the fact that contact angle is largely governed by the tendency for an oil to be excluded from the bilayer based on its size relative to the hydrocarbon chains of the lipids.[61] Thus, little difference was expected or observed for DIBs consisting of 16-carbon DPhPC tails or 18-carbon DOPC DIBs in hexadecane, a16-carbon alkane.

It is important to acknowledge the simplifications required for MD simulations. For instance, had we considered a liposome with 80 000 molecules instead of a 6-lipid micelle, the free energy profile for the lipid-in cases presented in Figure 3 could change due the possible difference in favorability and the number of lipids supplied per adsorption. In addition, the MD model disregards interactions between neighboring micelles (or inverse micelles) either in bulk or near the interface. Aggregation of inverse micelle due to aging or hydration could increase the stability of lipid structures in oil, thereby further reducing the rate of IFT reduction. The hydration level, which is defined as the number (#) of H_2O molecules inside an inverse micelle, and the number of lipids in a hydrated inverse micelle are also not considered. Finally, the curvature of the simulated oil−water interface is neglected since the droplets (ca. 1 mm diameter) exhibit curvature radii orders of magnitude higher than those of the lipids. Despite these choices, the MD simulations capture well the sustained energetic favorability between a partially packed monolayer and lipid-in micelles and the increasing difficulty of oil-bound inverse micelles to adsorb to a sparsely populated monolayer. These trends are in direct agreement with the kinetic processes observed experimentally for both lipid-in and lipid-out.

Considering the complexity involved in the lipid self-assembly process at an OW interface, applying simple concepts of first-order reaction kinetics and Henry's equation of state for an ideal scenario may not be suitable for accurately capturing the kinetics of the entire process. However, with a few valid assumptions, we demonstrate that this model could be used to determine the rate-limiting step involved in the monolayer formation process, and to compare the kinetics for surfactants approaching from different phases. The validity and limitations of our model are analyzed further in the SI.

CONCLUSIONS

The results from this study address what the required incubation times are for DPhPC and DOPC lipid-in (lipid-in-water) and lipid-out (lipid-in-oil) systems and the reasoning for longer incubation times and reduced rates of DIB formation success observed anecdotally for lipid-out DIBs formed using the lipid-out approach. Interfacial tension measurements indicate a simple adsorption controlled process for lipid-in assembly and predominantly adsorption-barrier controlled assembly for lipid-out systems after an initial period of simple adsorption. For lipid-out systems, we identify that the adsorption limitation becomes prevalent in the later stages of monolayer formation due to a high potential barrier for inverse micelle adsorption into a partially packed monolayer. This behavior creates an environment favorable for inverse micelle aggregation and tail−tail interactions in a way that is not seen in lipid-in systems due to the repulsive interaction between liposomes in water.[47] The formation of organogel in the subsurface is determined as a possible reason for this adsorption barrier. Results presented also clarify that advective

DOI: 10.1021/acs.langmuir.5b02293
Langmuir 2015, 31, 12883−12893

flow around the aqueous droplet helps achieve a tightly packed lipid monolayer by perturbing lipid structures in the subsurface and at the interface. Our experiments in general prove that a tightly packed monolayer with an equilibrium tension of ca. 1−2 mN/m, which is either achieved spontaneously by incubating droplets in quiescent oil or by applying advective flow to lipid-out mixtures, leads to higher DIB formation success rate. However, differences observed between rates of success for DIB formation for DPhPC and DOPC lipids suggest that other factors, including lipid shape and fluidity and even droplet size, also play roles in achieving a stable lipid bilayer between droplets.

■ ASSOCIATED CONTENT

Supporting Information

The Supporting Information is available free of charge on the ACS Publications website at DOI: 10.1021/acs.langmuir.5b02293.

Lipid-in solution preparation; lipid-out solution preparation; interfacial tension measurement; Figure S1, IFT data; DIB formation and contact angle measurement; electrical characterization of lipid bilayers; Figure S2, current-voltage curves; calculation of bilayer tension and adhesion energy for DIB; specific capacitance measurements; Figure S3, specific capacitance measurement procedure; MD simulation method; Figure S4, molecular dynamics system setup; Table S1, measured physical properties of DIBs; dynamic light scattering measurements of liposomes and inverse micelles; Figure S5, DLS measurements; additional IFT data for lipid-in and lipid-out conditions; Figure S6, interfacial tension versus time; interfacial tension measurement analysis; Figure S7, DPhPC-in surface pressure data and calculated fit; validity of model; Figure S8, comparison of experimental surface pressure and back-calculated surface pressure; limitations of model; Table S2, qualitative determination of suitable minimum lipid concentration; DOPC self-assembly free energy curves; Figure S9, free energy curves; and additional references (PDF)

■ AUTHOR INFORMATION

Corresponding Author

*E-mail: ssarles@utk.edu (S.A.S.).

Present Address

1512 Middle Dr., 414 Dougherty Engineering Building, Knoxville, TN 37996, U.S.A.

Notes

The authors declare no competing financial interest.

■ ACKNOWLEDGMENTS

The authors gratefully acknowledge financial support from Air Force Office of Scientific Research, Basic Research Initiative Grant Number FA9550-12-1-0464. Pendant drop measurements of interfacial tensions of lipid monolayers were conducted at the Center for Nanophase Materials Sciences, which is a DOE Office of Science User Facility.

■ REFERENCES

(1) Funakoshi, K.; Suzuki, H.; Takeuchi, S. Lipid Bilayer Formation by Contacting Monolayers in a Microfluidic Device for Membrane Protein Analysis. *Anal. Chem.* **2006**, *78* (24), 8169−8174.

(2) Sarles, S. A.; Madden, J. D. W.; Leo, D. J. Hair cell inspired mechanotransduction with a gel-supported, artificial lipid membrane. *Soft Matter* **2011**, *7* (10), 4644−4653.

(3) Holden, M. A.; Needham, D.; Bayley, H. Functional Bionetworks from Nanoliter Water Droplets. *J. Am. Chem. Soc.* **2007**, *129* (27), 8650−8655.

(4) Hwang, W. L.; Holden, M. A.; White, S.; Bayley, H. Electrical Behavior of Droplet Interface Bilayer Networks: Experimental Analysis and Modeling. *J. Am. Chem. Soc.* **2007**, *129* (38), 11854−11864.

(5) Castell, O. K.; Berridge, J.; Wallace, M. I. Quantification of Membrane Protein Inhibition by Optical Ion Flux in a Droplet Interface Bilayer Array. *Angew. Chem., Int. Ed.* **2012**, *51* (13), 3134−3138.

(6) de Planque, M. R. R.; Aghdaei, S.; Roose, T.; Morgan, H. Electrophysiological Characterization of Membrane Disruption by Nanoparticles. *ACS Nano* **2011**, *5* (5), 3599−3606.

(7) Bayley, H.; Cronin, B.; Heron, A.; Holden, M. A.; Hwang, W. L.; Syeda, R.; Thompson, J.; Wallace, M. Droplet interface bilayers. *Mol. BioSyst.* **2008**, *4* (12), 1191−1208.

(8) Hwang, W. L.; Chen, M.; Cronin, B.; Holden, M. A.; Bayley, H. Asymmetric Droplet Interface Bilayers. *J. Am. Chem. Soc.* **2008**, *130* (18), 5878−5879.

(9) Taylor, G. J.; Sarles, S. A. Heating-enabled formation of droplet interface bilayers using Escherichia coli total lipid extract. *Langmuir* **2015**, *31*, 325−325.

(10) Yanagisawa, M.; Yoshida, T.-a.; Furuta, M.; Nakata, S.; Tokita, M. Adhesive force between paired microdroplets coated with lipid monolayers. *Soft Matter* **2013**, *9* (25), 5891−5897.

(11) Leptihn, S.; Castell, O. K.; Cronin, B.; Lee, E.-H.; Gross, L. C. M.; Marshall, D. P.; Thompson, J. R.; Holden, M.; Wallace, M. I. Constructing droplet interface bilayers from the contact of aqueous droplets in oil. *Nat. Protoc.* **2013**, *8* (6), 1048−1057.

(12) Punnamaraju, S.; Steckl, A. J. Voltage Control of Droplet Interface Bilayer Lipid Membrane Dimensions. *Langmuir* **2011**, *27* (2), 618−626.

(13) Baret, J.-C.; Kleinschmidt, F.; El Harrak, A.; Griffiths, A. D. Kinetic Aspects of Emulsion Stabilization by Surfactants: A Microfluidic Analysis. *Langmuir* **2009**, *25* (11), 6088−6093.

(14) Zhang, F.; Proctor, A. Rheology and stability of phospholipid-stabilized emulsions. *J. Am. Oil Chem. Soc.* **1997**, *74* (7), 869−874.

(15) Aguiar, H. B. d.; Beer, A. G. F. d.; Strader, M. L.; Roke, S. The Interfacial Tension of Nanoscopic Oil Droplets in Water Is Hardly Affected by SDS Surfactant. *J. Am. Chem. Soc.* **2010**, *132* (7), 2122−2123.

(16) Thutupalli, S.; Fleury, J.-B.; Steinberger, A.; Herminghaus, S.; Seemann, R. Why can artificial membranes be fabricated so rapidly in microfluidics? *Chem. Commun.* **2013**, *49* (14), 1443−1445.

(17) Pichot, R.; Watson, R.; Norton, I. Phospholipids at the Interface: Current Trends and Challenges. *Int. J. Mol. Sci.* **2013**, *14* (6), 11767−11794.

(18) Sarles, S. A.; Stiltner, L. J.; Williams, C. B.; Leo, D. J. Bilayer Formation between Lipid-Encased Hydrogels Contained in Solid Substrates. *ACS Appl. Mater. Interfaces* **2010**, *2* (12), 3654−3663.

(19) Barriga, H. M. G.; Booth, P.; Haylock, S.; Bazin, R.; Templer, R. H.; Ces, O. Droplet interface bilayer reconstitution and activity measurement of the mechanosensitive channel of large conductance from Escherichia coli. *J. R. Soc., Interface* **2014**, *11* (98), 40410.1098/rsif.2014.0404.

(20) Hess, B.; Kutzner, C.; van der Spoel, D.; Lindahl, E. GROMACS 4: Algorithms for Highly Efficient, Load-Balanced, and Scalable Molecular Simulation. *J. Chem. Theory Comput.* **2008**, *4* (3), 435−447.

(21) Oostenbrink, C.; Villa, A.; Mark, A. E.; Van Gunsteren, W. F. A biomolecular force field based on the free enthalpy of hydration and solvation: The GROMOS force-field parameter sets 53A5 and 53A6. *J. Comput. Chem.* **2004**, *25* (13), 1656−1676.

(22) Darden, T.; York, D.; Pedersen, L. Particle mesh Ewald: An N·log(N) method for Ewald sums in large systems. *J. Chem. Phys.* **1993**, *98* (12), 10089−10092.

DOI: 10.1021/acs.langmuir.5b02293
Langmuir 2015, 31, 12883−12893

(23) Evans, D. J.; Holian, B. L. The Nose−Hoover thermostat. *J. Chem. Phys.* **1985**, *83* (8), 4069−4074.
(24) Hashimoto, M.; Garstecki, P.; Stone, H. A.; Whitesides, G. M. Interfacial instabilities in a microfluidic Hele-Shaw cell. *Soft Matter* **2008**, *4* (7), 1403−1413.
(25) Zhou, H.; Yao, Y.; Chen, Q.; Li, G.; Yao, S. A facile microfluidic strategy for measuring interfacial tension. *Appl. Phys. Lett.* **2013**, *103* (23), 234102−234102−4.
(26) Gruen, D. W. R.; Wolfe, J. Lateral tensions and pressures in membranes and lipid monolayers. *Biochim. Biophys. Acta, Biomembr.* **1982**, *688* (2), 572−580.
(27) Johnson, M. C. R.; Saunders, L. Time dependent interfacial tensions of a series of phospholipids. *Chem. Phys. Lipids* **1973**, *10* (4), 318−327.
(28) Walker, G. L. R. *Phosphatidylcholine Monolayer Formation at a Liquid−Liquid Interface as Monitored by the Dynamic Surface Tension*; Office of Naval Research: Department of Chemistry: Eugene, OR, 1998.
(29) Shchipunov, Y. A.; Kolpakov, A. F. Phospholipids at the oil/water interface: adsorption and interfacial phenomena in an electric field. *Adv. Colloid Interface Sci.* **1991**, *35* (0), 31−138.
(30) Vintiloiu, A.; Leroux, J.-C. Organogels and their use in drug delivery — A review. *J. Controlled Release* **2008**, *125* (3), 179−192.
(31) Walde, P.; Giuliani, A. M.; Boicelli, C. A.; Luisi, P. L. Phospholipid-based reverse micelles. *Chem. Phys. Lipids* **1990**, *53* (4), 265−288.
(32) Dixit, S. S.; Pincus, A.; Guo, B.; Faris, G. W. Droplet Shape Analysis and Permeability Studies in Droplet Lipid Bilayers. *Langmuir* **2012**, *28* (19), 7442−7451.
(33) Jarzynski, C. Nonequilibrium Equality for Free Energy Differences. *Phys. Rev. Lett.* **1997**, *78* (14), 2690−2693.
(34) Yasmann, A.; Sukharev, S. Properties of Diphytanoyl Phospholipids at the Air−Water Interface. *Langmuir* **2015**, *31* (1), 350−357.
(35) Song, Q.; Couzis, A.; Somasundaran, P.; Maldarelli, C. A transport model for the adsorption of surfactant from micelle solutions onto a clean air/water interface in the limit of rapid aggregate disassembly relative to diffusion and supporting dynamic tension experiments. *Colloids Surf., A* **2006**, *282−283* (0), 162−182.
(36) Rosen, M. J.; Hua, X. Y. Dynamic surface tension of aqueous surfactant solutions: 2. Parameters at 1 s and at mesoequilibrium. *J. Colloid Interface Sci.* **1990**, *139* (2), 397−407.
(37) Miller, R.; Joos, P.; Fainerman, V. B. Dynamic surface and interfacial tensions of surfactant and polymer solutions. *Adv. Colloid Interface Sci.* **1994**, *49* (0), 249−302.
(38) Moorkanikkara, S. N.; Blankschtein, D. New Methodology to Determine Equilibrium Surfactant Adsorption Properties from Experimental Dynamic Surface Tension Data. *Langmuir* **2009**, *25* (11), 6191−6202.
(39) Mitev, D. J.; Ivanova, T.; Vassilieff, C. S. Kinetics of lipid layer formation at interfaces. *Colloids Surf., B* **2002**, *24* (3−4), 185−192.
(40) Panaiotov, I.; Ivanova, T.; Balashev, K.; Proust, J. Spreading kinetics of dimyristoylphosphatidylcholine liposomes at the air/water interface below and above the main phase-transition temperature. *Colloids Surf., A* **1995**, *102* (0), 159−165.
(41) Walker, R. A.; Richmond, G. L. *Phosphatidylcholine Monolayer Formation at a Liquid:Liquid Interface as Monitored by the Dynamic Surface Tension 34*; Office of Naval Research, 1998.
(42) Eastoe, J.; Dalton, J. S. Dynamic surface tension and adsorption mechanisms of surfactants at the air−water interface. *Adv. Colloid Interface Sci.* **2000**, *85* (2−3), 103−144.
(43) Hamdaoui, O.; Naffrechoux, E. Modeling of adsorption isotherms of phenol and chlorophenols onto granular activated carbon: Part I. Two-parameter models and equations allowing determination of thermodynamic parameters. *J. Hazard. Mater.* **2007**, *147* (1−2), 381−394.
(44) Bleys, G.; Joos, P. Adsorption kinetics of bolaform surfactants at the air/water interface. *J. Phys. Chem.* **1985**, *89* (6), 1027−1032.
(45) Ariola, F. S.; Li, Z.; Cornejo, C.; Bittman, R.; Heikal, A. A. Membrane Fluidity and Lipid Order in Ternary Giant Unilamellar Vesicles Using a New Bodipy-Cholesterol Derivative. *Biophys. J.* **2009**, *96* (7), 2696−2708.
(46) Lindsey, H.; Petersen, N.; Chan, S. I. Physicochemical characterization of 1, 2-diphytanoyl-sn-glycero-3-phosphocholine in model membrane systems. *Biochim. Biophys. Acta, Biomembr.* **1979**, *555* (1), 147−167.
(47) Schneck, E.; Sedlmeier, F.; Netz, R. R. Hydration repulsion between biomembranes results from an interplay of dehydration and depolarization. *Proc. Natl. Acad. Sci. U. S. A.* **2012**, *109* (36), 14405−14409.
(48) Lin S.-Y.; Chang H.-C.; Chen E.-M. The Effect of Bulk Concentration on Surfactant Adsorption Processes—The Shift from Diffusion-Control to Mixed Kinetic-Diffusion Control with Bulk Concentration. *J. Chem. Eng. Jpn.* **1996**, *29* (4), 63410.1252/jcej.29.634.
(49) Danov, P. A. K.; Ivanov, B. Equilibrium and Dynamics of Surfactant Adsorption Monolayers and Thin Liquid Films. In *Handbook of Detergents*; Guy Broze: New York, 1999.
(50) Zhmud, B. V.; Tiberg, F.; Kizling, J. Dynamic Surface Tension in Concentrated Solutions of CnEm Surfactants: A Comparison between the Theory and Experiment. *Langmuir* **2000**, *16* (6), 2557−2565.
(51) Fainerman, V. B.; Zholob, S. A.; Miller, R.; Joos, P. Non-diffusional adsorption dynamics of surfactants at the air/water interface: adsorption barrier or non-equilibrium surface layer. *Colloids Surf., A* **1998**, *143* (2−3), 243−249.
(52) Schurtenberger, P.; Scartazzini, R.; Magid, L. J.; Leser, M. E.; Luisi, P. L. Structural and dynamic properties of polymer-like reverse micelles. *J. Phys. Chem.* **1990**, *94* (9), 3695−3701.
(53) Pautot, S.; Frisken, B. J.; Cheng, J.-X.; Xie, X. S.; Weitz, D. A. Spontaneous Formation of Lipid Structures at Oil/Water/Lipid Interfaces. *Langmuir* **2003**, *19* (24), 10281−10287.
(54) Ogino, K.; Onishi, M. Interfacial action of natural surfactants in oil/water systems. *J. Colloid Interface Sci.* **1981**, *83* (1), 18−25.
(55) Schindler, H. Exchange and interactions between lipid layers at the surface of a liposome solution. *Biochim. Biophys. Acta, Biomembr.* **1979**, *555* (2), 316−336.
(56) Mruetusatorn, P.; Boreyko, J. B.; Venkatesan, G. A.; Sarles, S. A.; Hayes, D. G.; Collier, C. P. Dynamic morphologies of microscale droplet interface bilayers. *Soft Matter* **2014**, *10* (15), 2530−2538.
(57) Thiam, A. R.; Farese, R. V., Jr.; Walther, T. C. The biophysics and cell biology of lipid droplets. *Nat. Rev. Mol. Cell Biol.* **2013**, *14* (12), 775−786.
(58) Gross, L. C. M.; Heron, A. J.; Baca, S. C.; Wallace, M. I. Determining Membrane Capacitance by Dynamic Control of Droplet Interface Bilayer Area. *Langmuir* **2011**, *27* (23), 14335−14342.
(59) Drexler, J.; Steinem, C. Pore-Suspending Lipid Bilayers on Porous Alumina Investigated by Electrical Impedance Spectroscopy. *J. Phys. Chem. B* **2003**, *107* (40), 11245−11254.
(60) Taylor, G. J.; Venkatesan, G. A.; Collier, C. P.; Sarles, S. A. Direct in situ measurement of specific capacitance, monolayer tension, and bilayer tension in a droplet interface bilayer. *Soft Matter* **2015**, *11* (38), 7592−7605.
(61) Needham, D.; Haydon, D. A. Tensions and free energies of formation of "solventless" lipid bilayers. Measurement of high contact angles. *Biophys. J.* **1983**, *41* (3), 251−257.

DOI: 10.1021/acs.langmuir.5b02293
Langmuir 2015, 31, 12883−12893